AVO processing of walkaway VSP data at Ross Lake heavy oilfield, Saskatchewan

Zimin Zhang, Robert R. Stewart, and Don C. Lawton

ABSTRACT

The AVO processing and analysis of walkaway VSP data at Ross Lake heavy oilfield, Saskatchewan is described in this report. A walkaway VSP geometry has advantages for AVO analysis: True amplitude processing is feasible and undesired wave-propagation effects can be minimized. At the top and the base of the target channel sand, the synthetic seismogram and walkaway VSP processing results show a similar amplitude variation with offset for the reflections of both PP and PS waves. These results indicate the promise of rock properties inversion using AVO gather from walkaway VSP.

INTRODUCTION

The Ross Lake heavy oilfield (operated by Husky Energy Inc.) is located in south-western Saskatchewan. The exploration target is the Cretaceous channel sand in the Cantuar Formation of the Mannville Group. Considering the advantages (FIG. 1) of using walkaway VSP data for AVO analysis, the walkaway VSP and multi-offset VSP were processed at the reservoir interval at the Ross Lake, Saskatchewan.

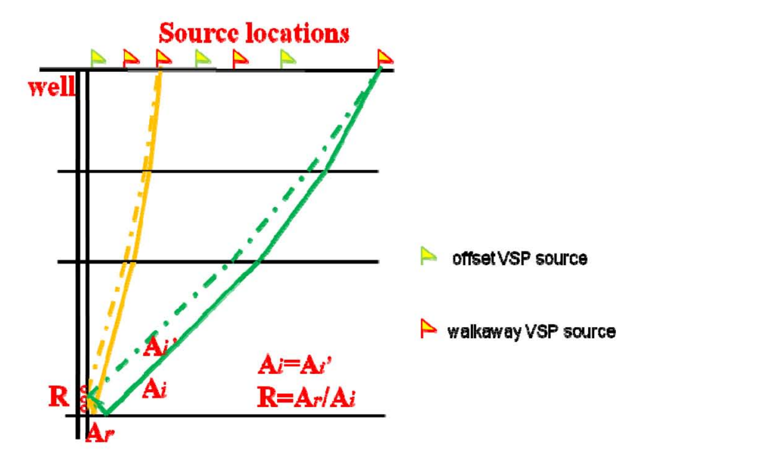

FIG 1. Schematic diagram of the advantage of walkaway VSP geometry for AVO processing. For the receivers very close to the reflectors, the incidence wave amplitude *Ai* approximately equal to the downgoing wave amplitude *Ai'*. Thus the reflectivity *R* can be calculated by dividing the upgoing wave amplitude *Ar* by downgoing wave amplitude *Ai*. Shots at varied locations give different incidence angles, therefore AVO gather can be built.

Table **1**. VSP surveys for walkaway VSP processing. The top processed receiver is 954m (above the Viking Formation). The top of the studied reservoir sand is approximately 1048m from the surface. The bottom receiver is in the channel sand.

Survey Type	*Source Offset (m)*	*Number of Receivers*	*Top Receiver Depth (m)*	*Bottom Receiver Depth (m)*	*Receiver Spacing (m)*
Zero Offset	54	130 (14)	197 (954.5)	1165	7.5 (15)
Offset	399	130 (14)	197 (954.5)	1165	7.5 (15)
	699	130 (14)	197 (954.5)	1165	7.5 (15)
Walk-away	150	14	954.5	1165	15
	250	14	954.5	1165	15
	558	14	954.5	1165	15
	997	14	954.5	1165	15

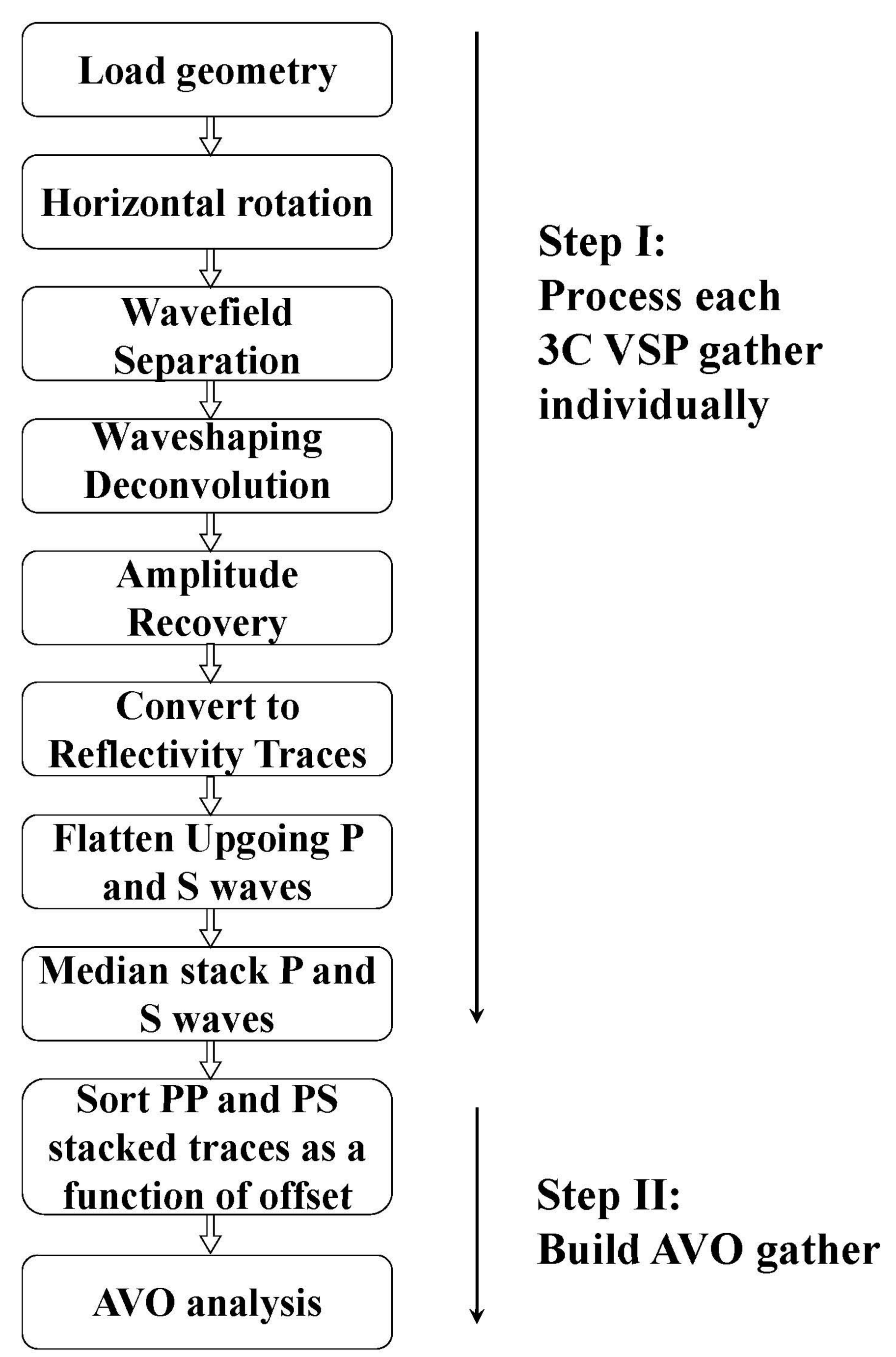

FIG 2. The walkaway VSP processing workflow for AVO analysis (modified after Coulombe et al., 1996). Each offset was processed individually to get a reflectivity trace from each shot, and then all shots were combined to form an offset-dependent gather for AVO analysis.

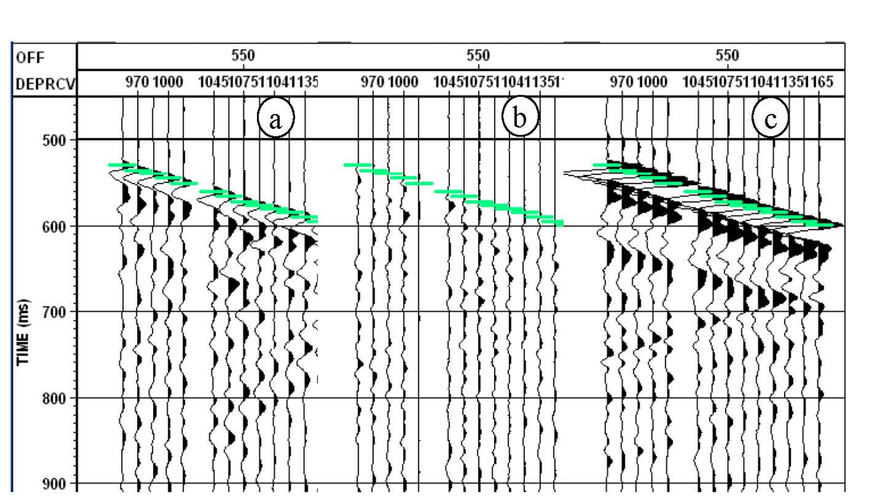

FIG 3. Hmax (a, horizontal radial), Hmin (b, horizontal transverse) after a horizontal rotation of X and Y components, and Z component data (c) of the offset 558 m shot (AGC applied, the green line is the first break picks).

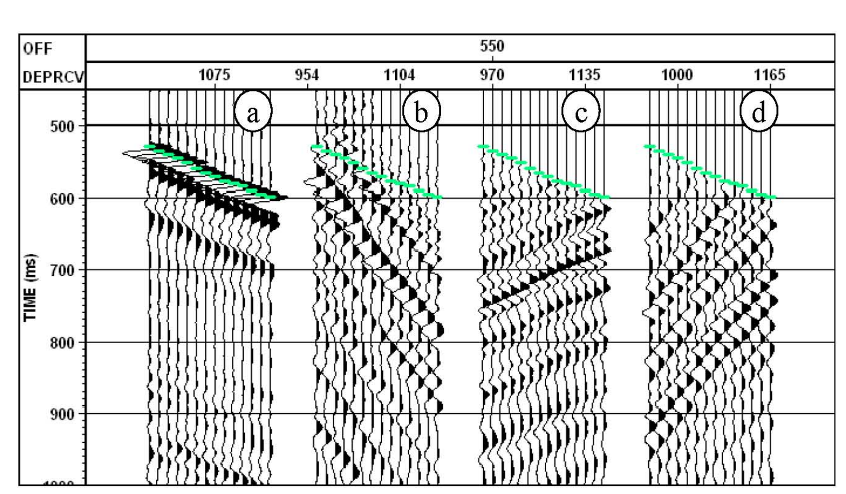

FIG 4. Downgoing P waves (a), downgoing SV waves (b), upgoing P waves (c), and upgoing SV waves (d) separated from Hmax and Z data of the offset 558 m shot (AGC applied, the green line indicates the first arrival picks).

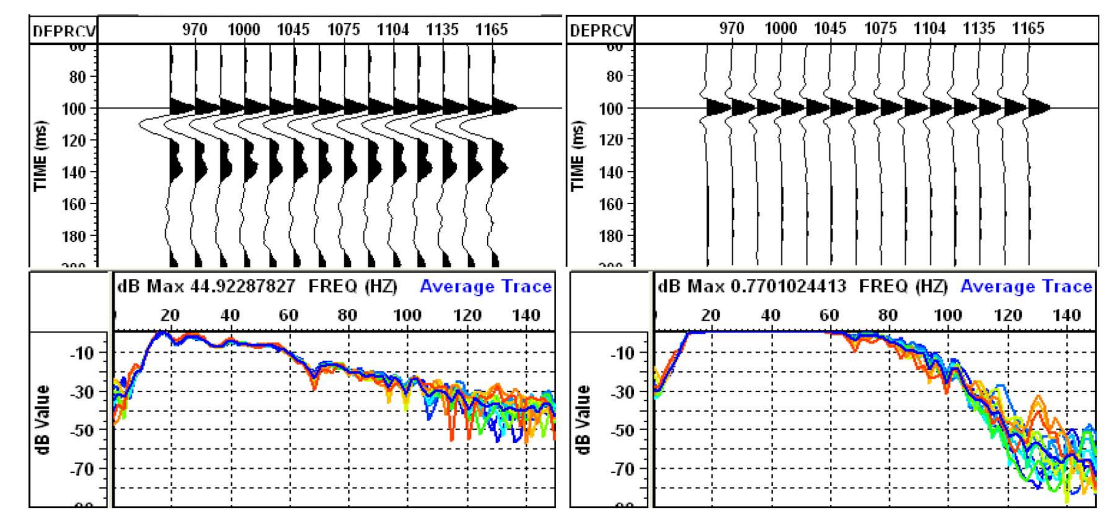

FIG 5. Downgoing P waves before (top left) and after (top right) deterministic deconvolution, as well as the corresponding amplitude spectra (the average spectrum is in blue) and average phase spectra (shot offset 558 m).

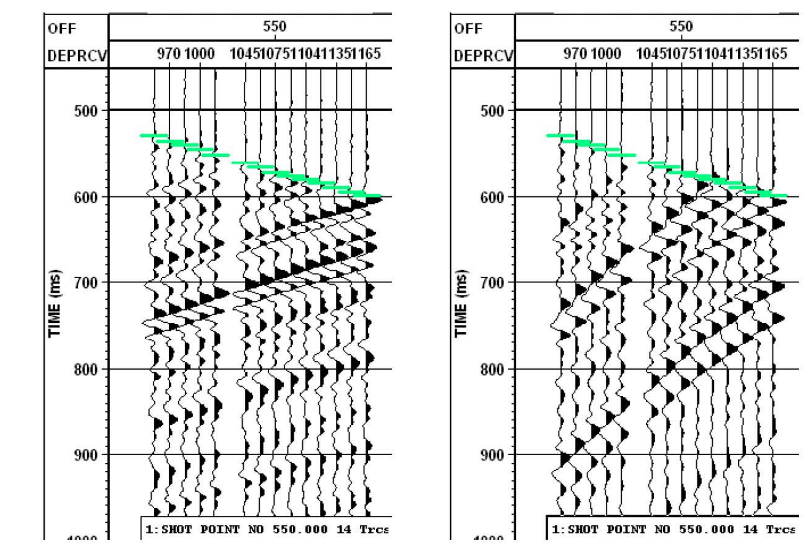

FIG 6. Upgoing P and SV waves after a deterministic deconvolution with operator derived from downgoing P waves (shot offset 558 m, the green line indicates first arrival picks).

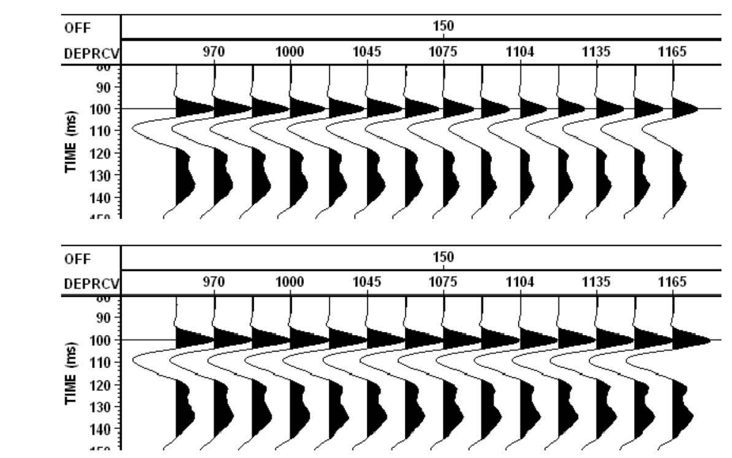

FIG 7. Downgoing P waves before and after mean scaling (flattened to 100 ms, shot offset 558 m). Note amplitude decay of direct P waves with increasing receiver depth before scaling.

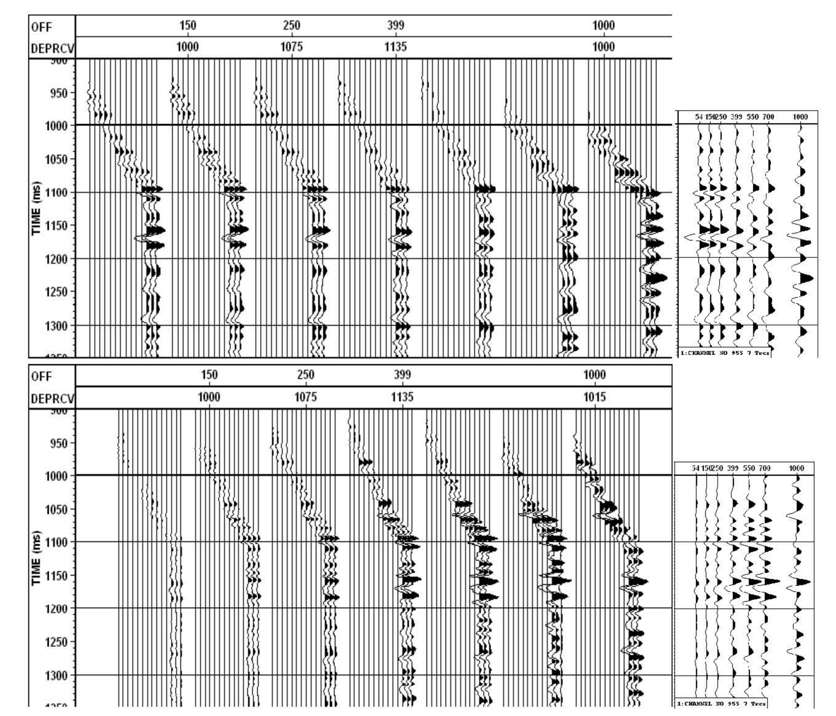

FIG 8. A 50 ms corridor mute to depth 1115m of upgoing P and upgoing SV waves, together with the resultant offset-dependent gathers of upgoing P and upgoing SV waves .

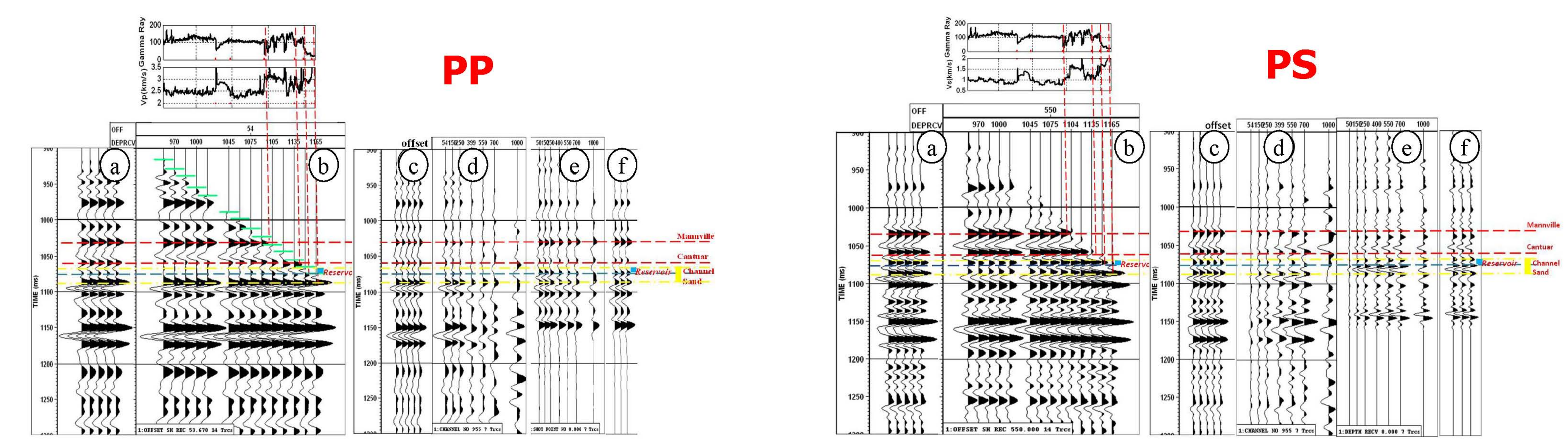

FIG 9. Correlation between well logs, zero-offset VSP within walkaway VSP receiver depth range (a: upgoing wave corridor stack; b: upgoing wave in two-way P traveltime (applied NMO and first-arrival time flattening)), and the comparison of offset gathers from walkaway VSP processing and synthetic seismogram from sonic and density logs for PP and PS waves (c: upgoing wave corridor stack of the zero-offset (54 m) VSP (repeated five times); d: offset gather from walkaway VSP; e: synthetic offset gather; f: stacked traces of the synthetic seismogram (repeated three times)).

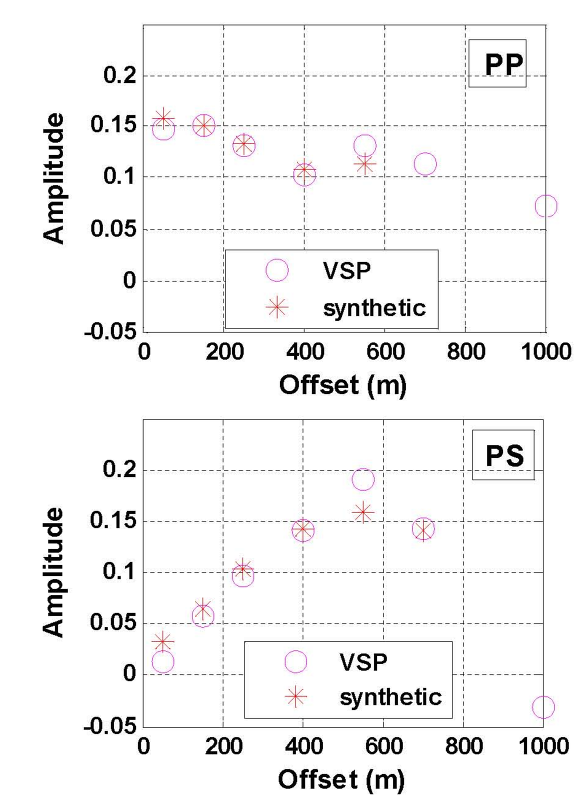

Offset (m) / Amplitude		50	150	250	400	550	700	1000
PP	VSP	0.147	0.15137	0.13118	0.10217	0.1313	0.11317	0.07217
	synthetic	0.1577	0.1510	0.1323	0.1082	0.1138	-	-
	mean difference (%)	0.18					-	
	standard deviation (%)	8.45					-	
PS	VSP	0.01303	0.05671	0.09677	0.14156	0.19037	0.14256	-0.0308
	synthetic	0.0326	0.0640	0.01035	0.1428	0.1578	0.1402	-
	mean difference (%)	-	-0.13					-
	standard deviation (%)	-	11.6					-

FIG 10. Comparison between the amplitude at the base of the channel sand from walkaway VSP and synthetic seismograms (generated by Syngram) for PP and PS data. The amplitude of synthetic data were scaled to the average amplitude level of VSP data.

CONCLUSION

A walkaway VSP geometry has advantages for AVO analysis. True amplitude recovery and wave propagation effects removal are feasible for walkaway VSP data. The use of corridor common-shot stack can improve the signal-to-noise ratio, and minimize undesired wave propagation effect at the same time. At the top and the base of the target channel sand, the synthetic seismogram and walkaway VSP processing results show comparable amplitude for both PP and PS waves. These results indicate the promise of rock properties inversion using AVO gather from walkaway VSP.

Estimating seismic attenuation (Qp & Qs) from rock properties

INTRODUCTION

As one of the basic attributes of seismic waves propagating in the earth, attenuation (or Q) has important values in the acquisition, processing, and interpretation of seismic data. In this report, the relationship between seismic attenuation and rock properties is investigated using VSP data and well logs from the Ross Lake heavy oilfield, Saskatchewan.

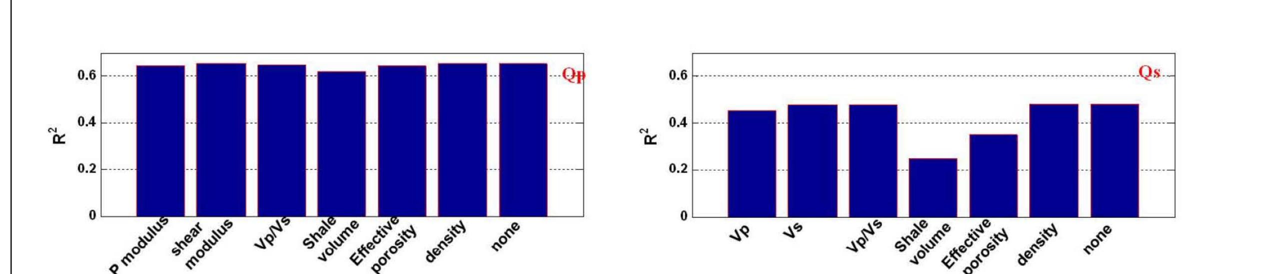

FIG 1. The influence of a single rock property value on prediction accuracy of Q value from rock properties. The prediction of Q value is from linear regression equation including all the 6 rock properties, except for the one noted right below the bar plot.

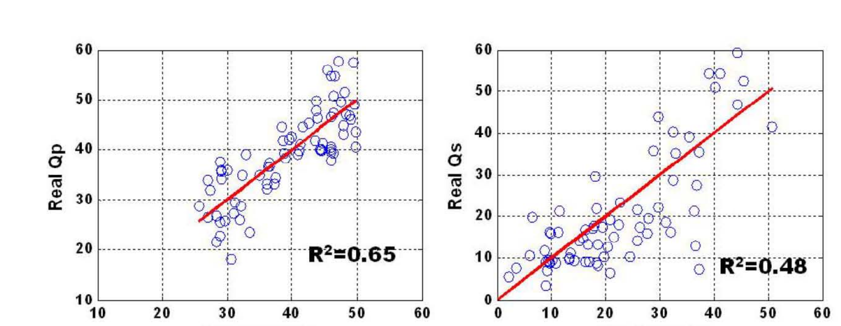

$$Qp = 1.95 * M - 13.63 * \frac{Vp}{Vs} + 37 * \emptyset + 21 * Vsh + 28.6$$

$$Qs = 66.4 * M - 13.38 * \frac{Vp}{Vs} + 285 * \emptyset + 101 * Vsh - 210$$

FIG 2. Comparison between real and predicted *Qp* and *Qs* values using the equations above.

CONCLUSION

The results reveal that Q values of P- and S-wave relate more to P modulus, Vp/Vs, effective porosity, and shale volume in the study area. The equations for Q estimation using these four rock properties were then derived using multiple parameter least-square regression method. The results show multiple rock properties have better prediction quality than a single rock property.

ACKNOWLEDGEMENTS

The authors would like to thank GEDCO for donating the VISTA processing package. The support by the sponsors of the CREWES project is gratefully appreciated.